Simulation of solar radiative transfer under different atmospheric conditions. Part II. Stochastic clouds

T.B. Zhuravleva

Institute of Atmospheric Optics,
Siberian Branch of the Russian Academy of Sciences, Tomsk

Received September 10, 2007

In memory of Georgii Aleksandrovich Titov, who would be 60 years old on March 5, 2008.

Author

Current models of stochastic clouds are briefly overviewed. Generalized formulas of the method of closed equations are presented; they are designed for calculation of mean fluxes and brightness fields in the statistically homogeneous model of broken clouds, taking into account the molecular absorption and interaction of radiation with aerosols and underlying surface. The approach is described, developed for reduction of the laboriousness of computations of mean spectral fluxes in the near-IR wavelength range 0.7–3.6 μm, which combines methods of closed equations and dependent tests. Mean flux calculations in the statistically homogeneous Poisson cloud model are compared with results of simulation in fractionally integrated cascade and Gaussian models of broken clouds, earlier validated against realistic subgrid-scale cloud structures.

Algorithms of the Monte Carlo method, designed for calculation of fluxes and brightness fields of the shortwave radiation in the deterministic atmosphere, both horizontally homogeneous and containing inhomogeneous clouds, were described in Part I of this paper.[1] Part II discusses the problems concerning the simulation of the solar radiation transfer in the presence of stochastic clouds. A brief description of certain most often used models of stochastic clouds is there presented. The main attention is devoted to the *statistically homogeneous* model of broken clouds, based on the *Poisson fluxes on the straight lines*; it was developed at IAO SB RAS under the leadership of G.A. Titov.

The algorithms of calculation of fluxes and brightness fields of solar radiation for the case of *isolated* broken clouds in the *absence of molecular absorption* were described earlier in Ref. 2. Part II presents generalized formulas for calculation of the average (over cloud realizations) radiation characteristics in the "aerosol – broken clouds – underlying surface" system. To decrease the laboriousness of the calculation algorithms for mean spectral radiative fluxes, taking into account the *molecular absorption*, a combination of the methods of dependent tests and closed equations is used. The paper presents approaches to comparison of radiative characteristics, calculated in the framework of different models of stochastic clouds: Poisson, Gaussian, and fractionally integrated cascade models, as well as discusses some results of the comparison.

1. Stochastic cloud models

As it was already noted earlier,[1] two- (2*D*) and three-dimensional (3*D*) cloud realizations can be obtained presently on the basis of the models, which can be separated conventionally into "physical" and "mathematical," in accordance with principles behind the simulation of mesoscale cloud fields. In classification of the existing mathematical models, we separate three groups:

– the Gaussian model (Yu.A.R. Mullamaa, B.A. Kargin, S.M. Prigarin, and A.N. Rublev);

– fractal cloud models, designed for imitation of complex geometrical shape of individual clouds (S. Lovejoy, A. Davis, P. Gabriel, D. Schertzer, G.A. Titov, and E.A. Babich) and simulation of liquid water path inside the overcast stratocumulus clouds (R. Cahalan, W. Wiscombe, A. Davis, A. Marshak, and others);

– the model on the basis of Poisson point fluxes in the space and on straight lines (G.A. Titov, G.N. Glazov, V.N. Skorinov, T.B. Zhuravleva, and E.I. Kassianov) and model, suggested by G. Pomraning, F. Malvadgi, R. Byrne, and R. Somerville.

Below, we give a brief description of the most often used cloud models.

1.1. The Gaussian model of broken clouds

Yu.A.R. Mullamaa and colleagues hypothesized that the cumulus clouds can be described on the basis of a stationary Gaussian process and created a theoretical-experimental model of the statistical structure of cumulus clouds.[3] *Numerical* models of the cloud structure, intended for simulation of cloud field realizations and calculation of the radiative characteristics, are designed by B.A. Kargin and S.M. Prigarin,[4] as well as by Rublev and coathors.[5,6]

0235-6880/08/03 163-13 $02.00

It is assumed that the cloud bottom boundary is defined by the plane $z = H_0$, while the cloud top boundary $z = w(x, y)$ is determined by the formula

$$w(x,y) = H_0 + \max\left[\left(|v(x,y)| - c\right), 0\right], \; c > 0,$$

where $v(x, y)$ is a homogeneous Gaussian field with zero mean, correlation function $K(x, y)$, and variance $\sigma^2 = K(0, 0)$. Selecting the input parameters c, σ, and $K(x, y)$, the Gaussian model can be quite readily adjusted in such a way as to obtain the required cloud fraction N and mean vertical and horizontal cloud sizes.

In the first numerical experiments for homogeneous isotropic fields the correlation function was determined as

$$K(x,y) = \sigma^2 J_0\left[\nu\left(x^2 + y^2\right)^{1/2}\right], \qquad (1)$$

J_0 is the Bessel function of first kind; ν is the parameter responsible for the horizontal cloud sizes, while the distribution of the geometrical cloud thickness $H = w(x, y) - H_0$ was described by the truncated Gaussian distribution. The shape of the H distributions was rigidly regulated by the model parameters, and the required mean $\bar{H}$ value could be reached only through scaling with the use of the parameter σ.[7] In such an approach, the difficulties were in the fact that with the use of $K(x, y)$ in the form of (1), the configurations of the cloud field had too "regular" structure and real distributions of the cloud thickness could substantially differ for the truncated Gaussian distributions (see Ref. 7 and the bibliography therein).

In this regard, S.M. Prigarin and A.L. Marshak[7] suggested a modification of the Gaussian model, which can be fitted to the results of the field observations. Input parameters of the modified model are the autocorrelation function of the cloud indicator field and distribution of the cloud field geometrical thickness. As satellite- and ground-based testing results have shown, the suggested method makes it possible to more adequately reproduce the real covariances of the cloud indicator field and distribution of its geometrical thickness; therefore, it is very promising for subsequent use.

The principles, outlined by Prigarin and Marshak[7] (preliminary simulation of the Gaussian field on the basis of discrete Fourier transform and subsequent nonlinear transform of the Gaussian field), were used by Evans and Wiscombe,[8] Venema et al.[9] for simulation of three-dimensional field of cloud liquid water content (LWC). Note that, in contrast to the Gaussian models, which construct only the cloud field *geometry*, methods by Evans and Wiscombe[8] and Venema et al.[9] make it possible to build the cloud indicator field, correlating with the *optical characteristics* of the cloud medium.

1.2. Fractal models

Recently, modelers develop a large class of fractal models, allowing them to take into account variations of some or another cloud characteristic (e.g., the geometrical shape or liquid water path (LWP)) in a wide range of scales.

For imitation of complex *geometrical shape* of real *cumulus* clouds, which can be considered as a fractal structure, special methods of simulation are used (see, e.g., Refs. 10 and 11). Models of cumulus clouds close to cascade ones, taking into account the random geometry of individual clouds, were suggested by E.A. Babich and G.A. Titov: the simulation uses the sum of n independent homogeneous isotropic Gaussian fields with decreasing variances and correlation radii.[2]

As the measurements show,[12–15] the distribution of liquid water inside marine stratocumulus clouds has the power-law spectrum

$$E(k) \propto k^{-\beta} \qquad (2)$$

as the spatial scale varies within, at least, three orders of magnitude (here $k = \pi/r$ is the wavenumber and r is the scale in km). Taking this circumstance into account, R. Cahalan, A. Davis, S. Lovejoy, A. Marshak, D. Schertzer, W. Wiscombe, and others suggested fractal models of spatial distribution of the LWP, which make it possible to preserve the liquid water balance within the *overcast* cloud layer (singular and bounded cascades, fractionally integrated cascade model[12–17]). Each model realization is determined by the mean optical depth $\bar{\tau}$ (optical depth is related to LWP by the well-known formula $\tau = (3LWP)/(2\rho r_{ef})$, ρ is the water density, and r_{ef} is the effective size of the cloud droplets), parameter p characterizing the variations of the optical depth σ_τ, and the exponent β [see Eq. (2)].

The advantage of the fractal models is in the fact that via varying a small number of relatively easily measured input parameters, it is possible to obtain different structures of the liquid water distribution, whose spatial correlations correspond to the observed ones. The fractal models of cumulus clouds are also suggested by A. Benassi and colleagues (tdMAP method[18]), F. Di Giuseppe and A. Tompkins,[19] and others (see also http://i3rc.gsfc.nasa.gov/Public_codes_clouds.htm).

The simulation of the cloud realizations, which somewhat adequately describes the real cloud fields, is the first step in the study of features of radiation transfer in stochastic clouds. The next step is the solution of radiative transfer equation (RTE), for which the spatial distribution of optical characteristics (the scattering and extinction coefficients and the scattering phase function) is determined by a particular realization of the cloud field.

For all of the above-mentioned physical and mathematical cloud models, the calculation of *statistical characteristics* of radiation is associated with the *numerical* RTE averaging whose essence lies in the simulation of a set of cloud realizations, RTE solution within each, and subsequent statistical processing of the calculated radiative characteristics. In such an approach, the computer time consumption depends significantly on the laboriousness of

construction of one realization. However, under certain physically based assumptions concerning the probabilistic properties of the cloud field, an *analytical* averaging of the radiative transfer equation is possible, which allows avoiding the simulation of many cloud realizations.

For the first time, one of the variants of such an approach for the broken clouds was formulated by Avaste and Vainikko.[20] The equations for the moments of intensity under different assumptions on the properties of the radiation field were obtained by different research groups; however, the models by Titov and Pomraning are presently in most common use.

1.3. Poisson model of broken clouds

One-layer *statistically homogeneous* model of broken clouds on the basis of Poisson fluxes of points on the straight lines was described by Zuev and Titov[2] in detail. In the framework of this model (henceforth referred to as "Poisson") the clouds are approximated by rectangular parallelepipeds with random horizontal sizes. The Poisson model is totally determined by the cloud fraction N, the geometrical cloud thickness H, and mean horizontal cloud size D; the input optical characteristics (extinction coefficient σ, single scattering albedo Λ, and scattering phase function in clouds) are assumed to be constant within all cloud elements and do not change from one cloud realization to another. When the geometrical cloud thickness H is fixed, the aspect ratio $\gamma = H/D$, more clearly characterizing the geometrical cloud field structure, is often used as the input parameter instead of the cloud diameter D.

Under the assumption that the n-dimensional probability of cloud presence is factorizable, G.A. Titov, together with G.N. Glazov and V.N. Skorinov, have obtained a closed system of equations for the *mean intensity* and developed efficient algorithms of the system solution by the Monte Carlo method of closed equations (MCE). The accuracy and applicability limits of these equations were compared with the corresponding calculations by the method of numerical simulation. The results of the comparison showed that the equations for the mean intensity are quite accurate and can be used for study of the influence of random geometry on the radiative properties of the broken clouds. The main advantage of MCE is that the *analytical* averaging, it rests upon, requires much less computation time as compared to the *numerical* RTE averaging.[2]

Let us present the relations, being the basis of simulation of mean fluxes and brightness fields under conditions of *isolated* broken clouds.[2] Consider a cloud layer occupying the height interval $H_0 = \{0, H\}$, and assume that the unit solar flux is incident on the top boundary H in the direction $\boldsymbol{\omega}_\odot = (\xi_\odot, \varphi_\odot)$. Average (over the set of cloud realizations) collision density, $f(\mathbf{x})$, satisfies the integral equation of the type [see Ref. 1, formula (3)] with the kernel

$$k(\mathbf{x}', \mathbf{x}) = \Lambda g(\mu) \sum_{i=1}^{2} D_i \eta_i \exp\{-\eta_i |\mathbf{r} - \mathbf{r}'|\} \times$$

$$\times \delta\{\boldsymbol{\omega} - (\mathbf{r} - \mathbf{r}')/|\mathbf{r} - \mathbf{r}'|\} \Big/ \left(2\pi |\mathbf{r} - \mathbf{r}'|^2\right) \qquad (3)$$

and the free term

$$\psi(\mathbf{x}) = \sum_{i=1}^{2} C_i \eta_i \exp\{-\lambda_i |\mathbf{r} - \mathbf{r}_H|\} \delta(\boldsymbol{\omega} - \boldsymbol{\omega}_\odot). \qquad (4)$$

Here $\mathbf{x} = (\mathbf{r}, \boldsymbol{\omega})$, $\boldsymbol{\omega} = (a, b, c)$ is the direction of photon travel after scattering at the point $\mathbf{r} = (x, y, z)$; $\mu = [\boldsymbol{\omega}', (\mathbf{r} - \mathbf{r}')] / |\mathbf{r} - \mathbf{r}'|$; $\mathbf{r}_H = \mathbf{r} + \boldsymbol{\omega}(z - H)/c$. Values of C_i, D_i, and η_i, $i = 1, 2$, are calculated by the formulas:

$$\eta_{1,2} = \left\{ \left(\sigma + A(\boldsymbol{\omega})\right) \mp \sqrt{\left[\sigma + A(\boldsymbol{\omega})\right]^2 - 4A(\boldsymbol{\omega}) N \sigma} \right\} \Big/ 2;$$

$$D_1 = (\eta_2 - \sigma)/(\eta_2 - \eta_1),\ D_2 = 1 - D_1, \qquad (5)$$

$$C_1 = (\eta_2 - \sigma N)/(\eta_2 - \eta_1),\ C_2 = 1 - C_1.$$

Value of $A(\boldsymbol{\omega})$ is determined from the relation:[21]

$$A(\boldsymbol{\omega}) = A_x |a| + A_y |b| + A_z |c|,$$

$$A_x = A_y = \left[1.65(N - 0.5)^2 + 1.04\right] / D,\ A_z = 0. \qquad (6)$$

Under assumption that the cloud optical characteristics are constant, the average intensity $\langle I(z, \boldsymbol{\omega}) \rangle$ can be represented in the form of the linear functional $J_h = (f, h)$ of the solution of the integral equation [see Ref. 1, formula (3)], taking into account Eqs. (3) and (4):

$$\langle I(z, \boldsymbol{\omega}) \rangle = \frac{\Lambda}{2\pi |c|} \int_{E_z} \sum_{i=1}^{2} D_i \exp\{-\eta_i |\mathbf{z} - \mathbf{z}'| / |c|\} \, \mathrm{d}z' \times$$

$$\times \int_{4\pi} g(\mu) f(z', \boldsymbol{\omega}') \, \mathrm{d}\boldsymbol{\omega}' + \langle j(z, \boldsymbol{\omega}) \rangle \delta(\boldsymbol{\omega} - \boldsymbol{\omega}_\odot), \qquad (7)$$

where

$$\langle j(z, \boldsymbol{\omega}) \rangle = \sum_{i=1}^{2} C_i \exp\{-\eta_i |z - H| / |c|\} \qquad (8)$$

is the average flux of the unscattered radiation.

To evaluate Eq. (7), it is possible to apply the general theory of Monte Carlo methods,[22] according to which J_h is determined by the mathematical expectation of the random quantity $\eta = \sum_{n=0}^{N_0} Q_n h(\mathbf{x}_n)$. From Eq. (7) it follows that the average intensity of radiation through the plane $z = z^*$ in the direction $\boldsymbol{\omega}^* \neq \boldsymbol{\omega}_\odot$ can be calculated provided at each point $\mathbf{x}_n = (\mathbf{r}_n, \boldsymbol{\omega}_{n-1})$ the quantity $Q_n h'(\mathbf{x}_n, \boldsymbol{\omega}^*)$ is calculated, where the weights Q_n are given by formula (15) from Ref. 1, and

$$h'(\mathbf{x}_n)=\begin{cases}\left[\sum_{i=1}^{2} D_i \exp\left\{-\eta_i\left|z^*-z_n\right|/\left|c^*\right|\right\} g(z_n,\mu_{n-1})\right]\Big/\left|c^*\right|, \\ \qquad (z^*-z_n)c^*>0,\ \ \mu_{n-1}=(\omega_{n-1},\omega^*), \\ 0, \qquad (z^*-z_n)c^*<0.\end{cases} \tag{9}$$

Average flux $\int_{4\pi} c\langle I(z,\omega)\rangle \mathrm{d}\omega$ through $z=z^*$ is also represented in the form of the linear functional of solution of equation [Ref. 1, formula (3)] with the weighting function of the form

$$h(\mathbf{x}_n)=\begin{cases}\sum_{i=1}^{2} D_i \exp\left\{-\eta_i\left|z^*-z_n\right|/\left|c_n\right|\right\},\ (z^*-z_n)c_n>0, \\ 0,\ (z^*-z_n)c_n<0.\end{cases} \tag{10}$$

Formulas (9) and (10) were obtained by assuming that the layer of the broken clouds is *isolated*. Appendix presents the extension of these formulas for the calculation of the average fluxes in the system "aerosol – broken clouds – underlying surface."[23]

Reference 24 presented the method of closed equations for the case of *two-layer* broken clouds under assumption that the random fields $\kappa_i(r)$, $i=1, 2$, constructed on the basis of Poisson flux of points on the straight lines, are independent and statistically homogeneous. (The assumption of independence of cloud fields is, as a rule, considered to be valid providing the clouds belong to different atmospheric levels: low, middle, and high). The developed algorithms make it possible to study the regularities of the radiative transfer in two-layer clouds and to estimate the applicability limits of the hypothesis on *random/maximum cloud overlap*, which is used in most (and, in particular, GCM) radiation codes.

At the same time, observations show that the presence (absence) of clouds within different cloud layers may be interrelated.[25] It is also well known that the clouds of one type (such as, *Altostratus* and *Altocumulus*) may be present simultaneously at different atmospheric levels, thus forming a multilayer (up to 4–6) system, in which the thickness of intercloud spaces range from a few tens of meters to one kilometer.

This circumstance stimulates the development of models designed for the description of the *correlated* cloud fields. One such model, representing a generalization of the Poisson cloud model,[26] uses as the input parameters the characteristics "responsible" for the correlation of the presence (or absence) of the cloud elements, belonging to different layers, and still being difficult to determine experimentally.

Note that the lack of information on the probabilistic characteristics of the spatial structure of the cloud field is a common problem in building and testing of new models. The recently observed interest in the complex studies of complex cloud systems and intense development of the physical cloud parametrizations (for example, in the framework of LES models) give promise to believe that this information will be obtained in the immediate future and, hence, more adequate models of the multilayer clouds will be constructed.

An ideologically close counterpart to the Poisson cloud model is the *non-constructive* model developed by G. Pomraning, F. Malvagi, R. Byrne, and R. Somerville (see, e.g., Refs. 27 and 28 among others). The system of equations with respect to the average intensity, obtained as a result of the *analytical averaging* of RTE, is solved by the discrete ordinate method. The input model parameters are LWP, the effective size of the cloud droplets r_{ef}, the cloud fraction N, the heights of the top and the bottom cloud boundaries, as well as the distribution density of horizontal cloud sizes and gaps between the clouds (clouds are approximated by ellipses). The dependence of the radiative characteristics on the cloud properties is discussed by Lane-Veron and Somerville.[29] The model validation is performed on the basis of data of Lane et al.[30]; the calculated and measured fluxes of the downward shortwave radiation were in best correspondence under the conditions when the cloud fraction varied in range 0.25–0.7, while clouds occupied relatively thin cloud layer. We note that the model, in which the state of the atmosphere was represented as a binary mixture, was also used by Valentyuk.[31]

2. Algorithms for calculation of statistical characteristics of broken clouds taking into account the molecular absorption

Methods of accounting for the absorption by the atmospheric gases within *one* spectral interval $\Delta\lambda$ under conditions of the *deterministic* atmosphere are described extensively [Ref. 1, section 4]. However, in computation of radiative characteristics for quite large set (a few tens or larger) of the spectral intervals N_{int}, it is advisable to use the *method of dependent tests* (MDT), whose essence is explained by Marchuk et al.[22] Below, we outline the modifications of MDT, developed by us for calculation of the *average* (over a set of cloud realizations) spectral fluxes of solar radiation in the near-IR spectral range (0.7–3.2 μm).[23] These algorithms are based on the Monte Carlo solution of the system of the closed equations for the mean intensity in the statistically homogeneous Poisson model of broken clouds; the molecular absorption is taken into account through the transmission function of atmospheric gases $T_{\Delta\lambda}(l)$ [Ref. 1, subsection 4.1]. The suggested MDT modifications were also used by us for calculation of radiative characteristics in the *horizontally homogeneous* model of clouds.

2.1. Simulation of average spectral fluxes of radiation taking into account the molecular absorption: benchmark algorithm and method of dependent tests

Let us present two algorithms designed for calculation of mean spectral radiation fluxes in the near-IR spectral region.

Algorithm 1 is based on the division of the entire considered spectral range into N_{int} intervals in accordance with the specified spectral resolution $\Delta\lambda$. In each interval, the optical characteristics of clouds and aerosol, as well as Rayleigh scattering coefficients are assumed to be constant. The mean fluxes through the plane $z = z^*$ are calculated in each interval independently according to the following scheme [Ref.1, subsection 4.1]:

– photon trajectories are simulated in the medium *without accounting for* the molecular absorption;

– the pathlength (or absorbing mass) is summed up along the photon trajectory until the collision at the point $\mathbf{r}_n$ [Ref. 1, formula (24)];

– at the collision point $\mathbf{r}_n$, the quantity $h_{z^*}(\mathbf{x}_n, \omega^*)T_{\Delta\lambda}(l^{(n)} + l)$ is calculated, where $l = |z_n - z^*|/|c_n|$ is the distance from the point $\mathbf{r}_n$ to the plane $z = z^*$ along the direction ω_n, while the function $h_{z^*}(\mathbf{x}_n, \omega^*)$ is defined by formula (10). (Formula (10) is used in calculations in isolated cloud layer and is given here just for simplicity of presentation. In fact, the calculations use generalizations of this formula to the case of the system "aerosol – broken clouds – underlying surface," presented in Appendix).

An obvious advantage of the algorithm 1 is in its ability to account for the spectral dependence of the optical parameters of clouds and aerosol in detail (for this reason, this method is considered as *benchmark*). At the same time, its obvious disadvantage is a considerable consumption of computer time for large values of N_{int}. For instance, for the spectral resolution $\Delta\nu \approx 10$–$20\ \text{cm}^{-1}$ the number of the intervals (and, correspondingly, the number of independent calculations on the basis of MDT) in the range 0.7–3.2 μm is ≈ 400.

Algorithm 2 is based on combination of the method of dependent tests[22] and the method of closed equations.[2] The mean collision density, satisfying equation [Ref. 1, formula (3)] with the kernel (3) and free term (4), as well as the weighting function (10), depend on the wavelength λ as the parameter. Obviously, the mth term of Neumann series [Ref. 1, formula (5)] can be written as follows:

$$(K_\lambda^m \psi_\lambda, h_\lambda) =$$

$$= \int_X \dots \int_X \prod_{i=0}^{m-1} k(\mathbf{x}_i, \mathbf{x}_{i+1}, \lambda) h(\mathbf{x}_m, \lambda) \psi(\mathbf{x}_0, \lambda)\, d\mathbf{x}_0 \dots d\mathbf{x}_m =$$

$$= \int_X \dots \int_X \psi(\mathbf{x}_0, \lambda_0) \frac{\psi(\mathbf{x}_0, \lambda)}{\psi(\mathbf{x}_0, \lambda_0)} h(\mathbf{x}_m, \lambda) \prod_{i=0}^{m-1} \tilde{k}(\mathbf{x}_i, \mathbf{x}_{i+1}, \lambda_0) \times$$

$$\times \frac{\prod_{i=0}^{m-1} k(\mathbf{x}_i, \mathbf{x}_{i+1}, \lambda)}{\prod_{i=0}^{m-1} \tilde{k}(\mathbf{x}_i, \mathbf{x}_{i+1}, \lambda_0)} d\mathbf{x}_0 \dots d\mathbf{x}_m, \qquad (11)$$

where $\psi(\mathbf{x}_0, \lambda_0)$ and $\tilde{k}(\mathbf{x}', \mathbf{x}, \lambda_0) = k(\mathbf{x}', \mathbf{x}, \lambda_0)/\Lambda(\lambda_0)$ are the initial and transitional probability densities of the Markovian chain for the wavelength λ_0, which will be called reference. Then, according to Ref. 22, the sought functional is defined by the formula of the type [Ref. 1, formula (8)]:

$$J_\lambda = M \sum_{n=1}^{N_0} Q_{n,\lambda}^* h(\mathbf{x}_n, \lambda) \qquad (12)$$

with auxiliary weights

$$Q_{0,\lambda}^* = \psi(\mathbf{x}_0, \lambda)/\psi(\mathbf{x}_0, \lambda_0),$$
$$Q_{n,\lambda}^* = Q_{n-1,\lambda}^* k(\mathbf{x}_{n-1}, \mathbf{x}_n, \lambda)/\tilde{k}(\mathbf{x}_{n-1}, \mathbf{x}_n, \lambda_0). \qquad (13)$$

With accounting for Eqs. (3) and (4) formulas (13) are transformed to the form

$$Q_{0,\lambda}^* = \sum_{i=1}^{2} \eta_i C_i \exp\{-\eta_i |\mathbf{r}_1 - \mathbf{r}_0|\} \Big/ \sum_{i=1}^{2} \eta_i^0 C_i^0 \exp\{-\eta_i^0 |\mathbf{r}_1 - \mathbf{r}_0|\},$$

$$Q_{n,\lambda}^* = \Lambda_\lambda Q_{n-1,\lambda}^* \sum_{i=1}^{2} \eta_i D_i \exp\{-\eta_i |\mathbf{r}_n - \mathbf{r}_{n-1}|\} g_{\lambda,n} \Big/ \qquad (14)$$

$$\Big/ \sum_{i=1}^{2} \eta_i^0 D_i^0 \exp\{-\eta_i^0 |\mathbf{r}_n - \mathbf{r}_{n-1}|\} g_{\lambda_0,n}.$$

Here $g_{\lambda,n} = g(\lambda, \mu_n)$; $\mu_n = (\omega_{n-1}, \omega_n)$; $\mathbf{r}_0$ and $\mathbf{r}_n$ are the points of entry and nth collision of the photon, respectively; D_i^0, C_i^0, and η_i^0 are the values of D_i, C_i, and η_i, given by formulas (5) at $\lambda = \lambda_0$, $i = 1, 2$.

Formulas (14) are quite cumbersome from the viewpoint of computational time: since the extinction coefficient $\sigma(\lambda)$ and the scattering phase function of clouds $g(\lambda, \mu)$ depend on the wavelength, at each step of the Markovian chain simulation it is necessary to simulate $2N_{\text{int}}$ exponential functions and N_{int} ratios $\{g_{\lambda,k}/g_{\lambda_0,k}\}$, $\lambda = \{\lambda_i,\ i = 1, \dots, N_{\text{int}}\}$ (or store the array of $\{g_{\lambda,k}/g_{\lambda_0,k}\}$, requiring quite large memory).

In the real liquid water clouds (in particular, cumulus clouds) the values of cloud *extinction coefficient* are quite large, while the fluctuations are not so considerable (about 10%, Fig. 1). Therefore, it can be expected that in formulas (14) the neglect of the spectral dependence of $\sigma(\lambda)$ is admissible.

The effect caused by the spectral dependence of the *scattering phase function* is associated with the dependence of the cloud single scattering albedo $\Lambda(\lambda)$ on the wavelength. In comparison with $\sigma(\lambda)$, $\Lambda(\lambda)$ depends on λ much stronger (see Fig. 1). For instance, the wavelength range 0.7–3.2 μm of our interest can be conventionally divided into 2 subintervals: 0.7–2.6 μm, where $\Lambda(\lambda)$ takes, predominately, quite high

values $\Lambda(\lambda) \geq 0.9$, and 2.7–3.2 μm, within which $\Lambda(\lambda) \approx 0.5$–0.6.

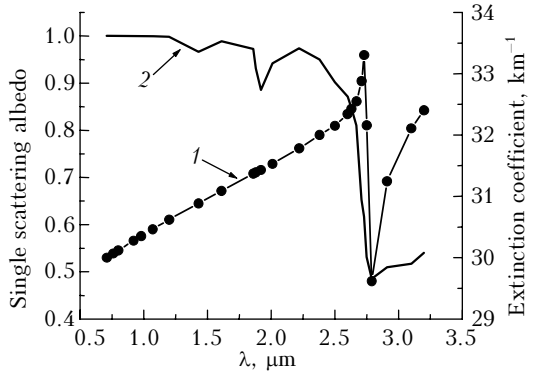

Fig. 1. The spectral behavior of extinction coefficient (*1*) and single scattering albedo (*2*) in clouds.

It is well known that the contribution of the *n*th order of scattering to the calculated radiative characteristic is proportional to $\Lambda^n(\lambda)$. When $\Lambda(\lambda)$ is not large, the contribution of the *n*th order of scattering rapidly drops and the radiation, transmitted and reflected by the clouds (especially albedo of the cloud layer) is formed mainly by a few first orders of scattering. In this regard, it can be speculated that the spectral dependence of $g_\lambda(\mu)$ is more significant in the subinterval 2.7–3.2 μm as compared to the subinterval 0.7–2.6 μm.

With the last circumstance in mind, we suggested MDT modifications, designed for calculation of mean fluxes in spectral subintervals 0.7–2.7 and 2.7–3.2 μm.

2.2. Numerical results

The cloud optical characteristics are calculated in accordance with the Mie theory[32] under assumption that the particle size distribution is approximated by the "wide" distribution of cloud droplets[33]; the refractive index of water was chosen in accordance with data from Ref. 34. The calculations were performed for *M* basic wavelengths whose values corresponded to local extrema of real and imaginary parts of the refractive index. For other wavelengths, the values of the optical characteristics were results of linear interpolation of the corresponding values, obtained for the basic set of wavelengths. The spectral behavior of the extinction coefficient and single scattering albedo of clouds is presented in Fig. 1.

The presented calculations take into account the absorption by water vapor and carbon dioxide on the basis of parameterizations of transmission functions, suggested in the works of B.M. Golubitskii, N.I. Moskalenko, and V.L. Fillipov and corresponding to the spectral resolution $\Delta\nu = 10$–$20\ \text{cm}^{-1}$ (see Refs. 35–37). The relative humidity stratification corresponded to mean-zonal models[38]; carbon dioxide was assumed to be uniformly mixed with a concentration of 330 ppm. The aerosol component and Rayleigh scattering were neglected; and surface albedo A_s was zero. Irrespective of the wavelength, the illuminance $E_0(\lambda)$ of the top boundary $H = 16$ km was 1: specification of radiative characteristics in relative units has made it possible to estimate the influence of *molecular absorption* of the atmosphere without accounting for the solar constant, which determines the contribution of a given spectral interval to the integrated characteristics.

Wavelength range 0.7–2.7 μm. The sensitivity of mean fluxes to spectral variations of the extinction coefficient and scattering phase function in clouds is estimated from comparing the calculated results, obtained with use of the algorithms 1 and 2. According to our hypothesis, formulas (14) are transformed as follows:

$$Q^*_{0,\lambda} = 1, \quad Q^*_{n,\lambda} = \Lambda(\lambda) Q^*_{n-1,\lambda}. \qquad (14')$$

(Hereinafter, the modification of MDT on the basis of Eqs. (14′) will be called the algorithm 2A). Analysis of results has shown that, in the wide variability range of the extinction coefficient, aspect ratio γ, and solar zenith angle $\xi_\odot$, the photon trajectory modeling can be made using one of the following scattering phase functions:

$$g_{\text{cl}}(\lambda,\mu) = \begin{cases} g_{\text{cl}}(\lambda_1,\mu), \lambda_1 = 0.708\,\mu\text{m}, \\ g_{\text{cl}}(\lambda_2,\mu), \lambda_2 = 2.503\,\mu\text{m}. \end{cases}$$

Mean fluxes of upward $F^{\uparrow}(z = H)$ and downward diffuse $F^{\downarrow}_s(z = 0)$ radiation, calculated with the use of the algorithms 1 and 2A, are presented in Table 1 together with the relative error $\delta RC^{(2A)}$, $RC = \{F^{\uparrow}(z = H),\ F^{\downarrow}_s(z = 0)\}$, which characterizes the accuracy of the algorithm 2A relative to the benchmark calculations:

$$\delta RC^{(2A)} = 100\% \left| \left\langle RC^{(1)} \right\rangle - \left\langle RC^{(2A)} \right\rangle \right| \Big/ \left\langle RC^{(1)} \right\rangle.$$

It follows from Table 1 that $\delta R^{(2A)}$ in the 0.7–2.6 μm subinterval is, on the average, within a relative calculation error of ≈3%. In the 2.6–2.7 μm subinterval, the cloud single scattering albedo rapidly drops (from 0.87 to 0.65, see Fig. 1), and the magnitude of $\delta F^{\uparrow,(2A)}(z = H)$ considerably increases, reaching ≈20% at $\lambda = 2.67$ μm. The value of $\delta F^{\downarrow,(2A)}_s$ $(z = 0)$ does not exceed the relative calculation error throughout interval 0.7–2.7 μm.

The performed analysis makes it possible to assess possibilities of using the algorithm 2A (formulas (14′)) for study of radiative characteristics in the cloudy atmosphere. If the *spectral* radiative fluxes are the subject of the study, then the accuracy of the suggested modification may turn to be unsatisfactory (in particular, this concerns interval 2.6–2.7 μm and, as it will be shown below, interval 2.7–2.8 μm). On the contrary, if we focus on the radiative characteristics *integrated* over a certain spectral interval, the use of the simpler algorithm 2A can be justified, because the contribution of the spectral interval to the total integrated quantity is determined by the weight of the solar constant, corresponding to this spectral interval.

Table 1. Results of calculations of mean fluxes of upward $F^{\uparrow}(z = H)$ and downward diffuse $F_s^{\downarrow}(z = 0)$ solar radiation on the basis of the algorithms 1 and 2A at the boundaries of the cloud layer and the corresponding relative errors of the algorithm 2A. $H = 0.5$ km, $D = 0.5$ km, $N = 0.5$, $\xi_{\odot} = 60°$, $\sigma(\lambda = 0.708\ \mu m) = 30\ km^{-1}$

λ, μm	$\langle F^{\uparrow,(1)}\rangle$	$\langle F^{\uparrow,(2A)}\rangle$	$\delta F^{\uparrow,(2A)}$, %	$\langle F_s^{\downarrow,(1)}\rangle$	$\langle F_s^{\downarrow,(2A)}\rangle$	$\delta F_s^{\downarrow,(2A)}$, %
0.708	0.393	0.393	0.0	0.386	0.386	0.0
0.760	0.383	0.395	3.1	0.374	0.363	3.0
0.797	0.395	0.405	2.5	0.382	0.370	3.1
0.917	0.311	0.317	2.9	0.294	0.285	3.0
0.980	0.365	0.366	0.3	0.342	0.332	2.9
1.070	0.401	0.405	1.0	0.379	0.369	2.6
1.202	0.299	0.295	1.3	0.271	0.264	2.6
1.426	0.384(−1)	0.380(−1)	1.0	0.303(−1)	0.289(−1)	4.0
1.613	0.336	0.329	2.8	0.292	0.295	1.0
1.863	0.125(−2)	0.122(−2)	2.4	0.680(−3)	0.690(−3)	1.5
1.875	0.214(−2)	0.203(−2)	5.0	0.120(−2)	0.112(−2)	7.0
1.920	0.200(−2)	0.206(−2)	3.0	0.117(−2)	0.113(−2)	3.4
2.020	0.162	0.168	3.7	0.132	0.143	7.5
2.224	0.270	0.250	7.0	0.220	0.243	9.0
2.383	0.171	0.166	2.9	0.139	0.141	1.4
2.503	0.180(−1)	0.182(−1)	1.1	0.126(−1)	0.126(−1)	0.0
2.600	5.64(−14)	5.98(−14)	6.0	1.80(−15)	1.78(−15)	1.0
2.634	3.52(−13)	3.75(−13)	6.5	1.48(−14)	1.55(−14)	4.6
2.670	1.01(−20)	1.20(−20)	20.0	5.42(−23)	5.35(−23)	1.3

Since the contribution of the solar constant to interval 2.0–3.0 μm is equal to ≈ 4.5%, the calculation error due to the use of Eqs. (14′) cannot significantly affect the integrated flux throughout spectral range 0.7–2.7 μm. At the same time, it is obvious that, from the viewpoint of computation effort, the algorithm 2A is more efficient than the algorithm 2, and moreover, than the algorithm 1.

Spectral range 2.7–3.2 μm. As it was noted above, the influence of the spectral dependence of the scattering phase function on the mean fluxes of solar radiation may appear more significant in this range than in range 0.7–2.7 μm. To test this hypothesis, we performed a series of calculations by applying the benchmark algorithm 1 and algorithm 2A with the use of the strongly different $g_{cl}(\lambda, \mu)$, as well as the algorithm 2B, in which the spectral behavior of $g_{cl}(\lambda, \mu)$ was taken into account and the spectral dependence of the extinction coefficient was neglected. According to Eqs. (14), the formulas for calculation by the algorithm 2B had the following form:

$$Q^*_{0,\lambda} = 1, \quad Q^*_{n,\lambda} = \Lambda_{\lambda} Q^*_{n-1,\lambda}\, g_{\lambda,n}/g_{\lambda_0,n}. \qquad (14'')$$

Due to the presence of the ratio $g_{\lambda,n}/g_{\lambda_0,n}$ in formula (14″), the selection of the reference wavelength λ_0, used for photon trajectory modeling, is especially important. The algorithm 2A is more efficient than 2B. However, the analysis of the simulation results has shown that it is impossible to select a universal scattering phase function for the algorithm 2A as it was done for spectral interval 0.7–2.7 μm. Therefore, the use of simplified formulas (14′) in the interval 2.7–3.2 μm was abandoned. At the same time, the results of the preliminary calculations show the ratio $g_{\lambda,n}/g_{\lambda_0,n}$ to be most close to 1 almost for all μ_n values at $\lambda_0 = 3.2$ μm, which, hence, was chosen as a reference wavelength in the algorithm 2B. The convergence of the algorithm 2B was ensured by the fact that in the considered wavelength range 2.7–3.2 μm, the cloud single scattering albedo $\Lambda_{cl} \approx 0.5$–0.6.

Results of calculations of the mean spectral fluxes with the use of the algorithms 1 and 2B, as well as the relative error of the algorithm 2B are presented in Table 2.

Table 2. Results of the calculations of the mean fluxes of upward $F^{\uparrow}(z = H)$ and downward diffuse $F_s^{\downarrow}(z = 0)$ solar radiation on the basis of the algorithms 1 and 2B at the boundaries of the cloud layer and the corresponding relative errors of the algorithm 2B. $H = 0.5$ km, $D = 0.5$ km, $\xi_{\odot} = 0°$, $\sigma(\lambda = 2.706\ \mu m) = 32.43\ km^{-1}$

λ, μm	$\langle F^{\uparrow,(1)}\rangle$	$\langle F^{\uparrow,(2B)}\rangle$	$\delta F^{\uparrow,(2B)}$, %	$\langle F_s^{\downarrow,(1)}\rangle$	$\langle F_s^{\downarrow,(2B)}\rangle$	$\delta F_s^{\downarrow,(2B)}$, %
2.706	0.142(−8)	0.141(−8)	0.7	0.351(−9)	0.365(−9)	4.0
2.728	0.137(−7)	0.122(−7)	10.9	0.938(−8)	0.959(−8)	2.2
2.750	0.108(−8)	0.969(−9)	10.6	0.102(−8)	0.103(−8)	1.0
2.796	0.197(−7)	0.178(−7)	6.8	0.430(−7)	0.398(−7)	7.4
2.906	0.130(−2)	0.126(−2)	3.1	0.352(−2)	0.342(−2)	2.8
3.095	0.261(−2)	0.260(−2)	0.5	0.527(−2)	0.53(−2)	0.5
3.200	0.131(−2)	0.129(−2)	1.5	0.173(−2)	0.175(−2)	1.2

The comparison of the calculations shows that the algorithm 2B is usable within the spectral interval 2.7–3.2 μm; more considerable deviations in the interval 2.73–2.79 μm do not have a significant effect on the calculation of integrated radiative fluxes in the wavelength range 2.7–3.2 μm.

The suggested approach was further used by us to calculate spectral fluxes in the wavelength range 0.7–3.6 μm.

3. On validation of Poisson model of broken clouds

A few stochastic models of the broken clouds, designed for the calculation of radiative characteristics of subgrid-scale cloud fields were described in subsection 2.1. The possibility of their application to study the process of radiative transfer in the broken clouds and parameterization of radiative properties of mesoscale cloud fields in the models of weather prediction and climate depends in many respects on results of the cloud model validation. The stochastic cloud models can be validated both on the basis of complex radiation measurements (see, e.g., Refs. 6, 30, and 39), and on the basis of other models, which already have passed validation (complete or partial) on realistic subgrid-scale spatial structures.[40,41]

At the initial stage of validation of the *Poisson* model of the broken clouds, we had relatively small amount of the experimental data. These data were not complex, i.e., the radiative, optical, and geometrical cloud characteristics were not always measured simultaneously. Nonetheless, the comparisons of the calculated statistical characteristics of clouds and radiation have shown that, on the whole, this model correctly describes the solar radiative transfer in the broken clouds.[42] This section describes an approach, suggested jointly by the author and A.N. Rublev and A.L. Marshak, which compares mean fluxes, calculated by the method of closed equations, with results of simulation in Gaussian and fractionally integrated cascade models.[43,44] Since two last models have been successfully validated through comparison with experimental data, we consider reasonable to use them for *indirect* validation of the Poisson model of broken clouds.

3.1. Fractionally integrated cascade cloud model

This model is designed for the simulation of the liquid water path *LWP* (or optical depth τ) distribution within the *overcast* marine stratocumulus clouds. The fractionally integrated cascade model was compared earlier both with additive fractal models (such as the model of generalized Brownian motion) and multiplicative fractal models (such as the model of bounded cascades[45]), which are used for simulation of horizontally inhomogeneous stratocumulus clouds, observed from satellites with high spatial resolution (of the type of LANDSAT). The results of the comparison have shown that in the framework of the simplest fractal models, which, in addition to the mean and standard deviation, also preserve the correlation properties of the simulated cloud field, the fractionally integrated cascade model most adequately describes fluctuations of the cloud optical depth.

Since at present there is no well-grounded theory of passage from $\tau(x, y)$ distribution in the overcast layer to the *broken* clouds $\tau_{bc}(x, y)$, to construct the "holes" in the cloud layer, we used the approach[46]:

$$\tau_{bc}(x, y) = b\max[\tau(x, y) - a, 0]. \qquad (15)$$

The choice of the "cutting" level $a = \text{cosnt} > 0$ is determined by one more input parameter of the cascade model, namely, the cloud fraction N. Restriction of the optical depth at the level $a > \tau_{min}$ has a consequence that the amount of liquid water in the layer decreases; to avoid this, the multiplication factor $b = \text{cosnt} > 0$ is introduced.

It was assumed that the cloud fields have dimensions 51.2×51.2 km, the number of pixels $N_{pix} = 2^9$ (which corresponds to pixel sizes of 0.1×0.1 km), the cloud geometrical thickness H is fixed, and the extinction coefficient is constant over the vertical $\sigma(z) = \sigma$. When constructing the realizations of the cascade model, the input parameters β and p were chosen within the range typical for marine stratocumulus clouds; here we present results, obtained at $\beta = 5/3$ and $p = 0.35$. All presented calculations are performed using the scattering phase function for $C1$ cloud ($\lambda = 0.69$ μm).[32]

We restrict our consideration to monochromatic radiation, because the passage to the frequency integrated radiative characteristics leads to increase of uncertainties, caused by the imprecision of parameterizations of cloud microphysical characteristics, inadequate atmospheric gas model and spectroscopic information, etc. The efficiency of calculations of the radiative characteristics, averaged over a set of realizations of the cascade model, was ensured through the use of the randomization procedure.[47]

The input parameters of Poisson and cascade cloud models were fitted based on two principal reasons. *First*, in order to account for the cloud optical depth variations within one cloud element during passage from one cloud realization to another, we suggested to average the results of the calculations in the Poisson ("pois") model with the use of a certain distribution density of the cloud optical depth $f(\tau)$:

$$\rangle RC(\gamma, N, \xi_\odot)\langle_{pois} = \int_0^\infty \langle RC(\tau, \gamma, N, \xi_\odot)\rangle_{pois} f(\tau)\,d\tau,$$

$$RC = F^\uparrow, F_s^\downarrow, F_d^\downarrow.$$

Here, the symbol $\rangle RC\langle_{pois}$ means that upward and downward (unscattered $F_d^\downarrow$ and diffuse $F_s^\downarrow$) radiative fluxes are averaged over a set of the cloud realizations $\langle RC\rangle_{pois}$ with a constant τ, as well as over a set of

possible values of the optical depth. The averaging procedure was performed by Zhuravleva and Marshak[43] with the use of the distribution density $f(\tau)$, which is modeled in the framework of the cascade model and satisfactorily agrees with gamma distribution, being a good approximation of the cloud optical depth distribution according to the data of satellite observations[48]:

$$f_\Gamma(\tau,\nu,\lambda) = (\lambda)^\nu \tau^{\nu-1}\exp(-\lambda\tau)/\Gamma(\nu), \quad \lambda = \nu/\bar{\tau},$$

$$\nu = \left(\bar{\tau}/\sigma_\tau\right)^2, \quad \sigma_\tau^2 = \nu/\lambda^2.$$

Second, the cloud aspect ratio γ was chosen in such a way as to match the unscattered radiation in the Poisson and cascade ("cas") models:

$$\left\langle F_d^\downarrow(\gamma,N,\xi_\odot)\right\rangle_{\text{pois}} = \left\langle F_d^\downarrow(N,\xi_\odot)\right\rangle_{\text{cas}}.$$

Note that the interrelation between $F_d^\downarrow$ and γ can be reliably determined at solar zenith angles $\xi_\odot \le 75°$ and the cloud amount $N < 0.7$. The *effective* value of γ, determined by the above-indicated method, may differ from its physical value $\gamma = H/D$. The question is raised as to how at such approach to the choice of the cloud aspect ratio the fluxes of *diffuse* radiation match each other in the cascade and Poisson models? The results of numerical simulation show[43] that the suggested approach:

1) ensures the coincidence of mean fluxes of diffuse radiation to within the relative error $\delta_{\text{pois}}F = 100\%(F_{\text{pois}} - F_{\text{cas}})/F_{\text{cas}} \le 3\%$ in a wide range of parameters of Poisson model and fractionally integrated cascade one. These discrepancies somewhat increase when the values of mean fluxes decrease (in particular, as $\bar{\tau}$ increases, $\delta_{\text{pois}}(F_s^\downarrow)$ grows by 10–20% as a function of cloud single scattering albedo Λ_{cl} (Fig. 2));

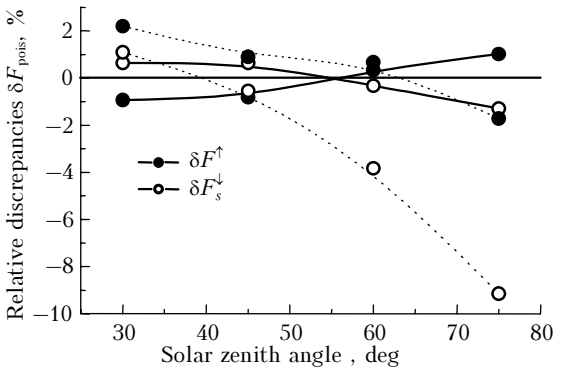

Fig. 2. Relative differences in the radiative fluxes, calculated in the cascade and Poisson cloud models: $N = 0.51$, $\bar{\tau} = 13$, $\sigma_\tau = 12.1$. Solid lines correspond to calculations at $\Lambda_{\text{cl}} = 1$ and dash lines at $\Lambda_{\text{cl}} = 0.95$.

2) makes it possible to use the same aspect ratio γ both in the case of conservative scattering and in the presence of moderate absorption ($\Lambda_{\text{cl}} \ge 0.95$). For fixed optical characteristics and cloud geometrical thickness, there exists a range $(\gamma_{\min}, \gamma_{\max})$ within which the mean flux calculation errors at all $0 \le \xi_\odot \le 75°$ do not exceed 5–10% in most cases.

3.2. Gaussian model

An approach to simulation of fluxes of the photosynthetically active radiation (PAR, 0.4–0.7 μm) was suggested[44] for fast calculations of monthly mean PAR fluxes as functions of the geographic latitude, month, and surface type. To calculate PAR under conditions of the horizontally homogeneous atmosphere, we used the method of direct simulation, while under broken cloud conditions – the benchmark algorithm described in Section 2. The transmission function of atmospheric gases was approximated by the exponential series; the molecular absorption coefficients were calculated on the basis of the spectroscopic HITRAN database taking into account the specified profiles of the meteorological parameters and atmospheric gas concentrations.

We used this approach when comparing mean fluxes of the upward and downward PAR, calculated in the Poisson and Gaussian cloud models. According to the obtained results,[6,39,49] the Gaussian model ensures a satisfactory agreement with the data of the ground-based and satellite radiation measurements when setting mean horizontal cloud size $D(N)$ and aspect ratio $\gamma = (N)$ determining the cloud top boundary $H_{\text{cl}}^{\text{top}}$, in accordance with data of Shmeter,[50] and with cloud extinction coefficient defined as[6,49]

$$\sigma_{\text{gaus}} = 30N. \qquad (16)$$

Based on the simulation results[44] it is found that, if the geometrical parameters in the Poisson model are set to be equal to those in the Gaussian model, and if the cloud extinction coefficient σ_{pois} is selected as directly proportional to the cloud fraction N according to the relation

$$\sigma_{\text{pois}} = 12N, \qquad (17)$$

then the PAR fluxes, calculated by the two models, well agree. Figure 3 presents *relative* differences in the upward and downward fluxes, calculated by the Gaussian and Poisson models:

$$\Delta RC = 100\%(RC_{\text{pois}} - RC_{\text{gaus}})/RC_{\text{gaus}},$$

$$RC = F^\uparrow, F_d^\downarrow, F_s^\downarrow.$$

For parameters specified in Fig. 3, the maximal discrepancy is observed for the flux of unscattered radiation $F_d^\downarrow$ and is approximately –30% for large solar zenith angles $\xi_\odot = 75°$, at small $F_d^\downarrow$ values. On the whole, the average discrepancy between PAR calculations by these models does not exceed 5 W/m^2 in most cases in a wide range of cloud amounts and solar zenith angles.

The difference in cloud extinction coefficient between Poisson and cascade models is caused by the fact that the clouds in the statistically homogeneous Poisson model are approximated by rectangular

parallelepipeds, while in Gaussian model the cloud shape is close to the truncated paraboloid. As a consequence, for the same value of σ the volume of the cloud matter will be larger in the Poisson model, and to compensate this, it is reasonable to reduce the value of σ_{pois}. The numerical factor in the relation $\sigma_{gaus} = 2.5\sigma_{pois}$ [see formulas (16) and (17)] is obtained by us via the additional calculations.

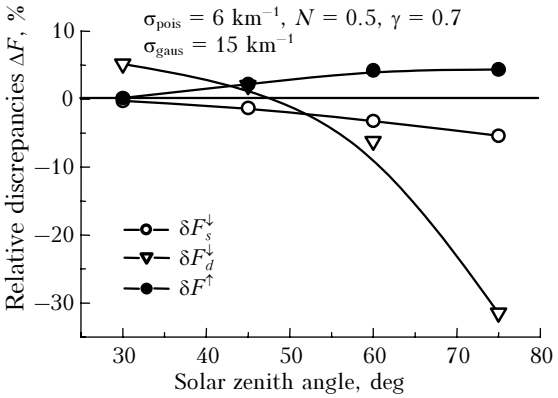

Fig. 3. Relative discrepancies of the fluxes of upward and downward radiation, calculated by the Gaussian and Poisson models. The height of the bottom boundary $H_{cl}^{bot} = 2$ km, the surface albedo is taken from Ref. 51 and corresponds to the coniferous forest.

The comparison of the measured and calculated monthly mean fluxes of downward PAR for BOREAS (BOReal Ecosystem-Atmosphere Study) NSA in 2001–2003 is given in Ref. 44. The comparison shows that, on the whole, the $F_{PAR}^{\downarrow}(z = 0)$ calculations are in good agreement with the experimental data.

Conclusion

The main results of the work are as follows:

1. The model of solar radiative transfer under different atmospheric conditions, including the *spatially inhomogeneous* and *stochastic* clouds has been developed. The average (over the cloud realizations) fluxes and brightness fields are calculated using an efficient method of closed equations, based on the analytical averaging of the radiative transfer equation in the framework of the statistically homogeneous Poisson cloud model.

In the algorithms of the statistical simulation, developed by us, the *molecular absorption* is accounted for either through the photon survival probability or using different parameterizations of the atmospheric gas transmission function. The computation scheme of accounting for the molecular absorption on the basis of the *k*-distribution method allows us to use in calculations the newest spectroscopic data, as well as the information on the device instrumental function, on actual meteorological profiles, and on the concentration of the atmospheric gases. To calculate a large amount of the *average* (over the cloud realizations) spectral fluxes and brightness fields, we developed an approach, combining the method of closed equations and method of dependent tests. To increase its efficiency in the near-IR range (0.7–3.6 μm), we proposed a MDT modification, based on the use of the specific features of the spectral dependence of the cloud characteristics in this spectral interval.

2. The computation algorithms, contained in the model, adequately describe the regularities of the transformation of the solar radiation in the clear sky and in the presence of the clouds. This is supported by:

– results of testing in the framework of the International Project Intercomparison of 3D Radiation Codes in the vertically and horizontally inhomogeneous realizations of the cloud fields, inferred from satellite and ground-based measurements;

– a good agreement of the spectral fluxes, calculated with benchmark line-by-line calculations and ground-based radiation measurements.

3. From comparison with the available data of the field measurements and results of the simulation by the fractionally integrated cascade and Gaussian models of the broken clouds, validated earlier against the realistic subgrid-scale cloud structures, it follows that the statistically homogeneous Poisson cloud model and the methods of calculation of statistical characteristics of solar radiation can be used for description of radiative transfer regularities in the actual cloud fields with the random geometry.

Acknowledgements

This work is partially supported by Russian Foundation for Basic Research (Grant No. 06–05–64484).

APPENDIX

Calculation of the mean intensity in the system "aerosol – broken clouds – underlying surface"

We present relations for calculation of mean fluxes; they are generalizations of formulas for an isolated cloud layer, presented in Subsection 1.3, to the case "broken clouds – aerosol – underlying surface."[23]

It follows from the radiative transfer equation linearity that accounting for the effect of the below- and above-cloud aerosol atmosphere, as well as the underlying surface, consists in the change of the boundary conditions for the mean intensity, written for isolated clouds. In particular, the radiation scattered by the aerosol in the beyond-cloud layers and reflected from the underlying surface can be considered as a certain diffuse source, which in the Monte Carlo calculations can be accounted for as follows.

Consider the cloudy – aerosol atmosphere, consisting of N_{lay} layers with the boundaries $\{H_j, H_{j+1}\}$, $j = 1, \ldots, N_{lay}$. Clouds occupy the layer with the number N_{cl} and with the top H_{cl}^{top} and bottom H_{cl}^{bot} boundaries, respectively: $H_{cl}^{top} = H_{N_{cl}+1}$, $H_{cl}^{bot} = H_{N_{cl}}$ (see Figure). Each *j*th aerosol layer is defined by the

extinction coefficient $\sigma_{a,j}$, single scattering albedo $\Lambda_{a,j}$, and scattering phase function $g_{a,j}(\mu)$. Denote through $\mathbf{r}_n^{(j)} = \mathbf{r}_n + \boldsymbol{\omega}_n(H_j - z_n)/c_n$ the point of crossing of the level H_j and the ray originating from the collision point $\mathbf{r}_n$ in the direction $\boldsymbol{\omega}_n$. In the vertically inhomogeneous aerosol atmosphere with piecewise constant extinction coefficient, the transmission function is defined by the formula

$$T\left(\mathbf{x}_n, \mathbf{r}_n^{(j)}\right) = \exp\left[-\tau\left(\mathbf{x}_n, \mathbf{r}_n^{(j)}\right)\right],$$

where the optical pathlength $\tau(\mathbf{r}_n, \mathbf{r}_n^{(j)})$ between the points $\mathbf{r}_n$ and $\mathbf{r}_n^{(j)}$ in the direction $\boldsymbol{\omega}_n$ is calculated by elementary formulas.

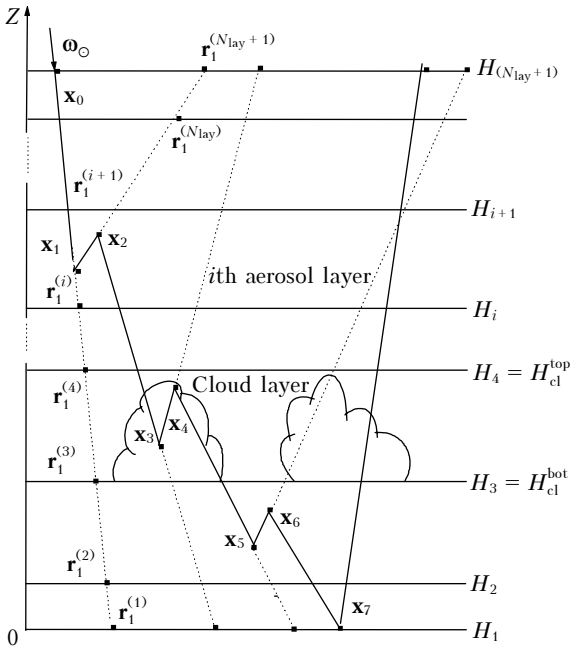

Fig. Schematic view of photon trajectory, demonstrating the contribution of the cloud layer and above – and below – cloud aerosol atmosphere to the values of the atmospheric radiative characteristics.

Write the function $h(\mathbf{x}_n)$ [see formula (10)] in the form, depending on the layer (number it with "i"), in which a collision occurred. For simplicity, we consider that the mean fluxes should be calculated at the levels, coinciding with the boundaries of the atmospheric model: $z_* = \{H_1, H_2, \ldots, H_{N_{lay}+1}\}$.

Scattering in the aerosol layer above the cloud layer

Upward flux. The function $h(\mathbf{x}_n)$ is determined by extinction only in the aerosol layers (point $\mathbf{x}_1 = (\mathbf{r}_1, \boldsymbol{\omega}_1)$ in Figure):

$$h(\mathbf{x}_n) = T\left(\mathbf{x}_n, \mathbf{r}_n^{(j)}\right), \quad i+1 \le j \le N_{lay}+1. \qquad \text{(A1)}$$

Downward flux. The function $h(\mathbf{x}_n)$ depends on the position of the level H_j (point $\mathbf{x}_2 = (\mathbf{r}_2, \boldsymbol{\omega}_2)$ in Figure).

The level H_j is within the above-cloud atmosphere (in particular, it may coincide with the cloud top boundary):

$$h(\mathbf{x}_n) = T\left(\mathbf{x}_n, \mathbf{r}_n^{(j)}\right), \quad N_{cl}+1 \le j \le i. \qquad \text{(A2)}$$

The level H_j belongs to the cloud layer (in a given case, it coincides with the cloud bottom boundary). In this case, the contribution to the downward flux is the extinction within the cloud layer plus the aerosol extinction of radiation, having reached the cloud top boundary without scattering:

$$h(\mathbf{x}_n) = T\left(\mathbf{x}_n, \mathbf{r}_n^{(N_{cl}+1)}\right)\sum_{i=1}^{2} D_i \exp\left\{-\eta_i \left|H_{cl}^{top} - H_{cl}^{bot}\right| / |c_n|\right\},$$
$$j = N_{cl}. \qquad \text{(A3)}$$

The level H_j belongs to the below-cloud atmosphere:

$$h(\mathbf{x}_n) = T\left(\mathbf{x}_n, \mathbf{r}_n^{(N_{cl}+1)}\right)\sum_{i=1}^{2} D_i \exp\left\{-\eta_i \left|H_{cl}^{top} - H_{cl}^{bot}\right| / |c_n|\right\} \times$$
$$\times T\left(\mathbf{r}_n^{(N_{cl})}, \mathbf{r}_n^{(j)}\right), \quad 1 \le j < N_{cl}. \qquad \text{(A4)}$$

Scattering in the cloud layer

Upward flux. The function $h(\mathbf{x}_n)$ depends on the position of the level H_j (point $\mathbf{x}_3 = (\mathbf{r}_3, \boldsymbol{\omega}_3)$ in Figure).

Level H_j is within the cloud layer (in a given case, it coincides with the cloud top boundary):

$$h(\mathbf{x}_n) = \sum_{i=1}^{2} D_i \exp\left\{-\eta_i \left|H_{cl}^{t} - z_n\right| / |c_n|\right\}, \quad j = N_{cl}+1. \qquad \text{(A5)}$$

The level H_j belongs to the above-cloud aerosol atmosphere:

$$h(\mathbf{x}_n) = \sum_{i=1}^{2} D_i \exp\left\{-\eta_i \left|H_{cl}^{top} - z_n\right| / |c_n|\right\} T\left(\mathbf{r}_n^{(N_{cl}+1)}, \mathbf{r}_n^{(j)}\right),$$
$$N_{cl}+1 < j \le N_{lay}+1. \qquad \text{(A6)}$$

Downward flux. The function $h(\mathbf{x}_n)$ depends on the position of the level H_j (point $\mathbf{x}_4 = (\mathbf{r}_4, \boldsymbol{\omega}_4)$ in Figure).

The level H_j is within the cloud layer (in this case, it coincides with the cloud top boundary):

$$h(\mathbf{x}_n) = \sum_{i=1}^{2} D_i \exp\left\{-\eta_i \left|H_{cl}^{bot} - z_n\right| / |c_n|\right\}, \quad j = N_{cl}. \qquad \text{(A7)}$$

The level H_j belongs to the below-cloud aerosol atmosphere:

$$h(\mathbf{x}_n) = \sum_{i=1}^{2} D_i \exp\left\{-\eta_i \left|H_{cl}^{top} - z_n\right| / |c_n|\right\} T\left(\mathbf{r}_n^{(N_{cl})}, \mathbf{r}_n^{(j)}\right),$$
$$1 \le j < N_{cl}. \qquad \text{(A8)}$$

Scattering in the below – cloud atmosphere

Upward flux. The function $h(\mathbf{x}_n)$ depends on the position of the level H_j (point $\mathbf{x}_5 = (\mathbf{r}_5, \omega_5)$ in Figure).

Level H_j is within the below-cloud atmosphere (in this case, it may coincide with the cloud bottom boundary):

$$h(\mathbf{x}_n) = T\left(\mathbf{x}_n, \mathbf{r}_n^{(j)}\right), \quad i+1 \le j \le N_{\text{cl}}. \tag{A9}$$

The level H_j belongs to the cloud layer (it coincides with the cloud top boundary):

$$h(\mathbf{x}_n) = T\left(\mathbf{x}_n, \mathbf{r}_n^{(N_{\text{cl}})}\right) \sum_{i=1}^{2} D_i \exp\left\{-\eta_i \left|H_{\text{cl}}^{\text{top}} - H_{\text{cl}}^{\text{bot}}\right| / |c_n|\right\}, \quad j = N_{\text{cl}} + 1. \tag{A10}$$

The level H_j belongs to the above-cloud atmosphere:

$$h(\mathbf{x}_n) = T\left(\mathbf{x}_n, \mathbf{r}_n^{(N_{\text{cl}})}\right) \sum_{i=1}^{2} D_i \exp\left\{-\eta_i \left|H_{\text{cl}}^{\text{top}} - H_{\text{cl}}^{\text{bot}}\right| / |c_n|\right\} \times \times T\left(\mathbf{r}_n^{(N_{\text{cl}})}, \mathbf{r}_n^{(j)}\right), \quad N_{\text{cl}} + 1 < j \le N_{\text{lay}} + 1. \tag{A11}$$

Downward flux. The function $h(\mathbf{x}_n)$ is determined by the extinction only in the aerosol layers (point $\mathbf{x}_6 = (\mathbf{r}_6, \omega_6)$ in Figure):

$$h(\mathbf{x}_n) = T\left(\mathbf{x}_n, \mathbf{r}_n^{(j)}\right), \quad 1 \le j \le i. \tag{A12}$$

Reflection from the underlying surface

In case of reflection from the underlying surface (point $\mathbf{x}_7 = (\mathbf{r}_7, \omega_7)$ in Figure), to calculate $h(\mathbf{x}_n)$, it is necessary to use formulas for the upward fluxes and introduce an additional weight $A_s/(2\pi)$.

References

1. T.B. Zhuravleva, Atmos. Oceanic Opt. **21**, No. 2, 81–95 (2008).
2. V.E. Zuev and G.A. Titov, *Atmospheric Optics and Climate* (Publishing house "Spektr" of IAO SB RAS, Tomsk, 1996), 271 pp.
3. Yu.-A.R. Mullamaa, M.A. Sulev, V.K. Pyldmaa, Kh.A. Okhvril, Kh.Yu. Niilisk, M.I. Allenov, L.G. Chubakov, and A.E. Kuusk, *Stochastic Structure of Cloud and Radiation Fields* (Academy of Sciences of Estonian Soviet Socialist Republic, Institute of Physics and Astronomy, Tartu, 1972), 281 pp.
4. B.A. Kargin and S.M. Prigarin, Atmos. Oceanic Opt. **7**, No. 9, 690–697 (1994).
5. A.N. Rublev and V.P. Golomolzin, *"Simulation of Cumulus Clouds,"* Preprint IAE-5567.16, Moscow (1992), 12 pp.
6. I.V. Geogdzhaev, T.V. Kondranin, A.N. Rublev, and N.E. Chubarova, Izv. Ros. Akad. Nauk, Ser. Fiz. Atmos. Okeana **33**, No. 5, 680–686 (1997).
7. S.M. Prigarin and A.L. Marshak, Atmos. Oceanic Opt. **18**, No. 3, 236–242 (2005).
8. K.F. Evans and W.J. Wiscombe, Atmos. Res. **72**, 263–289 (2004).
9. V. Venema, S. Meyer, S. Garcia, A. Knifka, C. Summer, S. Crewell, U. Lohnert, T. Trautmann, and A. Macke, Tellus **58A**, No. 1, 104–120 (2006).
10. E. Feder, *Fractals* (Mir, Moscow, 1991), 260 pp.
11. S. Lovejoy, Science **216**, No. 4542, 185–187 (1982).
12. R.F. Cahalan, W. Ridgway, W.J. Wiscombe, T.L. Bell, and J.B. Snider, J. Atmos. Sci. **51**, 2434–2455 (1994).
13. R. Cahalan and J. Snider, Remote Sens. Environ. **28**, 95–107 (1989).
14. A. Davis, A. Marshak, W. Wiscombe, and R. Cahalan, J. Atmos. Sci. **53**, No. 11, 1538–1558 (1996).
15. A. Marshak, A. Davis, W. Wiscombe, and R. Cahalan, J. Atmos. Sci. **54**, No. 11, 1423–1444 (1997).
16. S. Lovejoy, A. Davis, P. Gabriel, D. Schertzer, and G.L. Austin, J. Geophys. Res. D **95**, No. 8, 11699–11715 (1990).
17. R. Cahalan and J. Joseph, Mon. Weather Rev. **117**, No. 2, 261–272 (1989).
18. A. Benassi, F. Szczap, A. Davis, M. Masbou, C. Cornet, and P. Bleuyard, Atmos. Res. **72**, Nos. 1–4, 291–315 (2004).
19. F. Di Giuseppe and A. Tompkins, J. Atmos. Sci. **60**, No. 15, 1774–1794 (2003).
20. O. Avaste and G. Vainikko, *Calculation of the Mean Values of Intensities and Fluxes in Broken Clouds,* IAMAP/IAGA International Union of Geodesy and Geophysics, XV General Assembly (Moscow, 1971), 24 pp.
21. T.B. Zhuravleva and G.A. Titov, in: *Statistical Characteristics of Unscattered Radiation in Cumulus Clouds. Optical and Meteorological Studies of the Atmosphere* (Nauka, Novosibirsk, 1987), 108–119 pp.
22. G.I. Marchuk, G.A. Mikhailov, M.A. Nazaraliev, R.A. Darbinyan, B.A. Kargin, and B.S. Elepov, *Monte Carlo Method in the Atmospheric Optics* (Nauka, Novosibirsk, 1976), 280 pp.
23. G.A. Titov, T.B. Zhuravleva, and V.E. Zuev, J. Geophys. Res. D **102**, No. 2, 1819–1832 (1997).
24. G.A. Titov and T.B. Zhuravleva, Atmos. Oceanic Opt. **12**, No. 3, 196–203 (1999).
25. I.P. Mazin and A.Kh. Khrgian, eds., *Clouds and the Cloudy Atmosphere. Handbook* (Gidrometeoizdat, Leningrad, 1989), 647 pp.
26. S.M. Prigarin, T.B. Zhuravleva, and P.V. Volikova, Atmos. Oceanic Opt. **15**, No. 10, 832–838 (2002).
27. F. Malvagi and G. Pomraning, Atmos. Oceanic Opt. **6**, No. 9, 1064–1090 (1993).
28. F. Malvagi, R.N. Byrne, G. Pomraning, and R.C.J. Somerville, J. Atmos. Sci. **50**, No. 14, 2146–2158 (1993).
29. D. Lane-Veron and R. Somerville, J. Geophys. Res. **109**, D18113, doi: 10.1029/2004JD004524 (2004).
30. D. Lane, E. Goris, and R. Somerville, J. Climate **15**, No. 20, 2921–2933 (2002).
31. A.N. Valentyuk and G.K. Predko, *Optical Image in Remote Observation* (Nauka i Tekhnika, Minsk, 1991), 359 pp.
32. D. Deirmendjian, *Electromagnetic Scattering on Spherical Polydispersions* (Elsevier, 1969), 290 pp.
33. E.M. Feigelson, ed., *Radiation in the Cloudy Atmosphere* (Gidrometeoizdat, Leningrad, 1981), 280 pp.
34. V.E. Zuev, *Propagation of Visible and Infrared waves in the Atmosphere* (Sovetskoe Radio, Moscow, 1970), 495 pp.
35. B.M. Golubitskii and N.I. Moskalenko, Izv. Akad. Nauk SSSR, Ser. Fiz. Atmos. Okeana **IV**, No. 3, 346–359 (1968).
36. N.I. Moskalenko, Izv. Akad. Nauk SSSR, Ser. Fiz. Atmos. Okeana **V**, No. 11, 1179–1190 (1969).

37. V.L. Fillipov Izv. Akad. Nauk SSSR, Ser. Fiz. Atmos. Okeana **IX**, No. 7, 774–775 (1973).
38. V.E. Zuev and V.S. Komarov, *Statistical Models of Temperature and Atmospheric Gas Constituents* (Gidrometeoizdat, Leningrad, 1986), 264 pp.
39. N.E. Chubarova, A.N. Rublev, A.N. Trotsenko, and A.N. Trembach, Izv. Ros. Akad. Nauk, Ser. Fiz. Atmos. Okeana **35**, No. 1, 222–239 (1999).
40. G.W. Petty, J. Atmos. Sci. **59**, No. 20, 2910–2929 (2002).
41. E. Kassianov, T.P. Ackerman, R. Marchand, and M. Ovtchinnikov, J. Quant. Spectrosc. and Radiat. Transfer **77**, No. 4, 395–416 (2003).
42. T.B. Zhuravleva and G.A. Titov, Issled. Zemli iz Kosmosa, No. 5, 81–87 (1989).
43. T.B. Zhuravleva and A.L. Marshak, Izv. Ros. Akad. Nauk, Ser. Fiz. Atmos. Okeana **41**, No. 6, 783–797 (2005).
44. T.B. Zhuravleva, A.N. Rublev, T.A. Udalova, and T.Yu. Chesnokova, Atmos. Oceanic Opt. **19**, No. 1, 57–61 (2006).
45. R.F. Cahalan, Nonlin. Processes in Geophys. **1**, No. 1, 156–167 (1994).
46. A. Marshak, A. Davis, W.J. Wiscombe, W. Ridgway, and R.F. Cahalan, J. Climate 11, No. 3, 431–446 (1998).
47. G.A. Mikhailov, *Weighting Monte Carlo Methods* (Publishin House of SB RAS, Novosibirsk, 2000), 247 pp.
48. H. Barker, B. Wielicki, and L. Parker, J. Atmos. Sci. **53**, No. 16, 2304–2316 (1996).
49. V.V. Trembach, A.N. Rublev, and T.A. Udalova, in: *IRS 2000: Current Problems in Atmospheric Radiation,* W.L. Smith and Yu.M. Timofeyev, eds., (A. Deepak Publishing, Hampton, Virginia, 2001), pp. 1058–1060.
50. S.M. Shmeter, *Thermodynamics and Physics of Convective Clouds* (Gidrometeoizdat, Leningrad, 1987), 288 pp.
51. S.J. Hook, ASTER Spectral Library: Johns Hopkins University (JHU) spectral library; Jet Propulsion Laboratory (JPL) spectral library; The United States Geological Survey (USGS-Reston) spectral library. 1998. Dedicated CD-ROM. Version 1.2.